Biol. Cybern. 91, 63–75 (2004)
DOI 10.1007/s00422-004-0500-8

Biological Cybernetics

An adaptive neuro-fuzzy method (*ANFIS*) for estimating single-trial movement-related potentials

D. D. Ben Dayan Rubin[1,2], **G. Baselli**[1], **G. F. Inbar**[2], **S. Cerutti**[1]

[1] Department of Biomedical Engineering, Politecnico di Milano, 20133 Milano, Italy
[2] Department Electrical Engineering, Technion, Israel Institute of Technology, 32000 Haifa, Israel

Received: 22 July 2002 / Accepted: 22 June 2004 / Published online: 21 August 2004

Abstract. This study aims to recover transient, trial-varying evoked potentials (EPs), in particular the movement-related potentials (MRPs), embedded within the background cerebral activity at very low signal-to-noise ratios (SNRs). A new adaptive neuro-fuzzy technique will attempt to estimate movement-related potentials within multi-channel EEG recordings, enabling this method to completely adapt to each input sweep without system training procedures. We assume that one of the sensors is corrupted by noise deriving from other sensors via an unknown function that will be estimated. We will approach this problem by: (1) spatially decorrelating the sensors in the preprocessing phase, (2) choosing the most informative of the filtered channels that will permit the best MRP estimation (input-selection phase) and (3) training the neuro-fuzzy model to fit the noise over the chosen sensor and therefore estimating the buried MRP. We tested this framework with simulations to validate the analytical results before applying them to the real biological data. Whenever it is applied to biological data, this method improves the SNR by more than 12 dB, even to very low SNRs. The processing method proposed here is likely to complement other estimation techniques and can be useful to process, enhance and analyse single-trial MRPs.

Keywords: Movement-related-potential – Single-trial estimation – Nonlinear estimation methods – Evoked potentials – Neuro-fuzzy models

1 Introduction

When approaching the problem of analysing evoked potentials (EPs) or event-related potentials (ERPs), two major issues arise. The first issue stems from the extremely low signal-to-noise ratio (SNR) with overlapping spectra of the evoked response embedded within the background EEG brain activity, ranging from 0 to -20 dB, depending on the type of evoked signals. The second one concerns possible vectorial signal summation, resulting in component overlap, which may cause partial or total occlusion of the desired features. Usually these field potentials are averaged to increase the SNR and other phase-locked EEG activity. The averaging methods do not take into account that in single epochs response activity may vary widely in both time course and scalp distribution (Popivanov and Krekule 1983), depending on the external experimental conditions as well as on the subject's performance and state of mind (Schwent and Hillyard 1975). Single-trial-analysis methods can avoid problems due to time and/or phase shifts and can potentially reveal richer information about event-related brain dynamics. On the other hand, these methods suffer from pervasive artefacts associated with blinks, eye movements, muscle noise and SNR arising from the fact that non-phase-locked background EEG activities often are larger than phase-locked response components. The focus of this study deals with recovering specifically movement-related potentials (MRPs); nevertheless the proposed methodology can be applied generally to ERP estimations. The movement potentials relate to the planning and execution of voluntary movements (Boschert and Deecke 1986) and have usually been studied in the context of simple movements, commonly of single limbs (Deecke et al. 1976). Many of the studies address the focus on MRPs because of their importance in both clinical and research purposes. Many algorithms have been proposed to detect trial-to-trial variability (Bartnik et al. 1982; Birch et al. 1993; Thakor 1993). Most of these algorithms work well for cognitive evoked potentials with a non-negative SNR but fail whenever applied to MRPs that have a highly negative SNR. The few algorithms that succeed in these cases of highly negative SNR have to rely heavily on the average MRP (Lange et al. 1997; Cerutti et al. 1988). Other works investigate the use of physiological signals, usually from multi-electrode EEG, for communication and operation of devices for both healthy subjects and patients with severe motor impairments in many international groups (Birbaumer et al.

Correspondence to: D. B. D. Rubin
(e-mail: dbd@biomed.polimi.it)

1999; Babiloni et al. 2000; Pfurtscheller et al. 2000; Wolpaw and McFarland 1994). This alternative communication channel is called in the literature brain–computer interface (BCI). Other studies address the problem of detecting asynchronous motor control (Mason and Birch 2000), or rather the problem of classifying different MRPs, whether detected (Levine et al. 1999; Müller-Gerking et al. 1999).

In this paper, we propose a novel method that is likely to complement other techniques for estimating EPs and to enhance BCI (detection and classification) procedures. For this kind of application, together with other clinical-surgical ones, the number of electrodes must be limited to enhance computational capabilities and to provide simpler interfaces for easier implementation. The problem of recovering the MRP embedded within the ongoing cerebral activity has been approached step by step developing three serial processing phases: a spatial filtering stage, an *input selection* unit and a noise canceller block. From a set of eight EEG leads we obtain four spatially decorrelated channels by means of discrete Laplace filtering. We assume that the MRP signal is mainly located over one of the four channels that will be referred to as *primary input* in the sense of Widrow's *noise cancelling* technique. By contrast, the other three remaining channels are supposed to carry mostly background activity (noise in our problem) and, accordingly, are the *reference* inputs for *noise cancellation* from the *primary input*. An adaptive neuro-fuzzy inference system (*ANFIS*) network is used to adaptively estimate the relationship between the *reference* inputs and noise component of the *primary input*. The *input selection* phase starts by testing four different *noise cancelling* models, each one with a different channel playing the role of *primary input*. Each model is adapted over two iteration cycles of *ANFIS*, thereby obtaining a first approximation (mainly linear) of the respective *noise cancelling* rule. The selection procedure chooses as the most representative channel the one that (at this early stage of adaptation) has the largest component not explained by the *reference* inputs. After the selection only the chosen model is further trained in order to optimize the *noise cancellation*. The final residual is considered a single sweep estimate of the MRP, which is thus obtained without any a priori information or template, preventing distortions due to fitting procedures and enhancing sensitivity to the MRP dynamics. Both the last two stages, *channel selection* and *noise cancelling*, exploit the *ANFIS* capabilities of tracking both non-linearity and linearity in multi-dimensional input spaces (Jang 1993). *ANFIS* enables the proposed method to serve as a fast convergent estimating procedure that enables on-line processing. Using the same architecture for the MRP estimation, this study, unlike previous approaches, leads also to a classifier of the sensor that possesses higher information content regarding the burring noise among the others in multi-electrode EEG recordings. This paper focuses on presenting the architecture of the proposed method, providing simulations to ascertain its viability, and finally applying it to a biological data set for testing the MRP estimations.

2 Methods

2.1 Experimental setup

Two male subjects, right-handed and aged 29 and 26 years, not suffering from neurological or muscular disorders, participated in this study. Informed consent was obtained from both subjects. The subjects sat on a chair with palms lying on a table and feet on a footstool. Micro-switches were placed under both right and left index fingers and both right and left big toes. The task was to press the four micro-switches randomly – self-pacing – as briefly as possible, pausing for approximately 3 s between two consecutive presses, keeping the eyes opened and trying to minimize blinking. Electro-oculographic (EOG) artefacts were not rejected. Cortical potentials were recorded with electrodes placed over Fp1, Fp2, F3, F4, C3, C4, T3 and T4, all *reference*d to an electrode placed over Cz. A flexible cap (Electro-CapTM), on which the electrodes are permanently installed according to the 10–20 placement system, was worn by the subjects and strapped to the chest to eliminate movement-related artefacts. The electrodes were Ag-AgCl surface electrodes, circular, with a 6-mm diameter. Cross impedances were kept strictly below 5 KΩ. The state of the four micro-switches was recorded in order to synchronize events in the EEG with external events. The EEG channels were amplified using a custom-made optically isolated amplifier with a gain of 10^4 and a $\{0, 40\}$ Hz low-pass filter. The amplifier had input impedances consisting of a resistive component on the order of 200 MΩ; thus the maximum signal loss was 0.0025%. The amplified signals were digitized and sampled, together with the micro-switches' states, at 250 Hz. All the computation processing were done on the data off-line using Matlab. Each recording session lasted 10 min. The data were divided into single trials from 1.5 s before the movement of the micro-switch and until 1 s after it (for a total of 625 samples). The movements of the same type were collected and rearranged, obtaining for each subject four sets of movements: (1) left hand movements, (2) right index finger movements, (3) left big toe movements and (4) right big toe movements.

2.2 Laplacian spatial filtering

We apply the Laplacian filter (Müller-Gerking et al. 1999; Babiloni et al. 2000; Millàn et al. 2002; Nunez et al. 1994; McFarland et al. 1997) to enhance the SNR, to completely discard *reference* effects, and to obtain partial spatial decorrelation of the available channels (Nunez 1981), although the number of electrodes used in this study is small for the filter application. Before applying the filter, the position of the electrode sites was projected over a planar surface, and the resulting data points were interpolated assuming the propagation of the electric field monotonically decreasing as the radius increased from each electrode site (proportional to inverse radius–inverse distance among the location of the eight sites). The obtained surface approximated a surface described using a higher number of electrodes (Fig. 1). The filter, applied to the interpolated plane, took at any instant of time eight

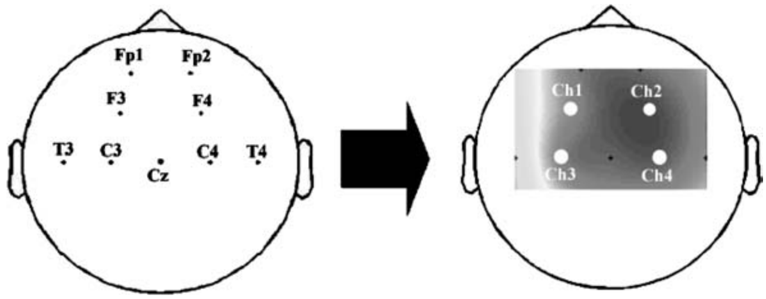

Fig. 1. Location of the eight electrodes used for recording on the left. All electrodes were *referenced* to Cz. The surface interpolation, on the right, provides the Laplacian filtering with samples over the eight directions of the square filtering mask. *White circles* indicate the position of the four filtered channels that will be used henceforth as the referring channels

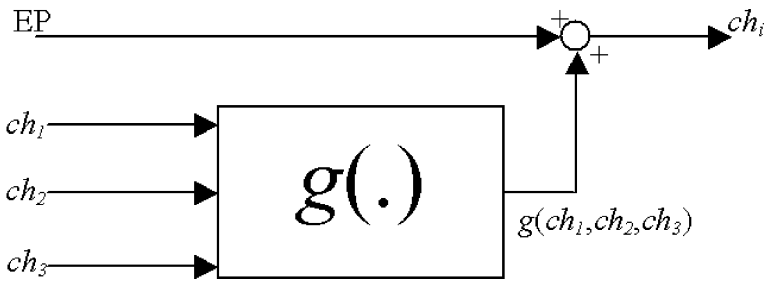

Fig. 2. Model of interfering noise sources (ch_1, ch_2, ch_3) via $g(\bullet)$ (linear/highly nonlinear function) that corrupt additively the EP to generate channel ch_i. Channel ch_i is the selected channel that best describes this relation: EP+ $g(ch_1, ch_2, ch_3) = ch_i$

samples located over the diagonal and vertical–horizontal edges of a square and subtracted their average from the sample placed over the centre of the square. The filtering square was chosen to minimize the distance between the interpolated sample and the nearest data sample. The filter was centred over sites F3, F4, C3 and C4 because they were better wrapped by the other border electrodes; hereafter they will be identified by the nos. 1, 2, 3, 4, respectively.

2.3 Model of channel relationship

In the present study we assume that all channels but one are useful for tracking the noise found in the last channel. Let **Ch** be the set containing *n* channels (raw vectors) used for the recording: $\mathbf{Ch} = \{ch_1, ch_2, \ldots, ch_n\}$; let ch_i be the *i*th element of that set which is considered the *primary input* (i.e. signal plus noise); let $\mathbf{Ch}_i^*$ be the subset obtained from the set **Ch**, removing element ch_i: $\mathbf{Ch}_i^* = \mathbf{Ch} - \{ch_i\}$, which is considered the *reference* input set (i.e. set containing mainly the noise signals). $\mathbf{Ch}_i^*$ contains local measurements of the electric fields generated by the underlying noise generators. These signals are subject to different transformations while affecting ch_i. We investigate a way to correlate $\mathbf{Ch}_i^*$ to the noise present over the sensor ch_i. Let $g(\bullet)$ be the unknown function that relates the elements of $\mathbf{Ch}_i^*$ to ch_i. The model of this relationship is shown in Fig. 2 (in the particular case of four sensors of this study) and is represented by:

$$ch_i = g_i(\mathbf{Ch}_i^*) + Signal\,, \tag{1}$$

where $g_i(\mathbf{Ch}_i^*)$ identifies the noise over ch_i and $Signal$ is the embedded signal (i.e. the EP). $\mathbf{Ch}_i^*$ and ch_i are supposed to obey the following hypotheses: (1) $\mathbf{Ch}_i^*$ is a set of decorrelated noise signals and (2) ch_i is assumed to be the signal that contains both the information regarding the function $g_i(\bullet)$ and the embedded signal to recover. Based on these assumptions we processed the signals using the "*adaptive noise cancelling*" of Widrow and Stearns (1985) – see appendix for details. This adaptive method is modified by substituting the classical adaptive linear block with an adaptive linear/nonlinear method, *ANFIS*, estimating via successive iterations $g(\bullet)$. The first iteration steps are used to select ch_i among all possible input combinations (see Sect. 2.4 for details). Generally, the use of Widrow's filtering relies on adaptive linear techniques, and the use of *ANFIS* (see appendix for details) can extend the class that searches the g function even to nonlinear spaces.

2.4 Input selection procedure

Once the four-signal output is given, we need to obtain heuristically an order of priority of these potential inputs, and then we can use them accordingly. *ANFIS* employs an efficient hybrid learning method that combines the gradient descent and the least-squares (LS) methods. As a result, *ANFIS* can usually generate satisfactory results right after the first epochs of training, that is only after the first applications of the LS method. Since the LS method is computationally efficient, we can construct *ANFIS* models for various combinations of inputs, train them with few applications of the hybrid method and then choose the one with the best performance and proceed for further training. The proposed *input selection* method is based on the assumption that the *ANFIS* model with the smallest root mean squared error (RMSE) after a few epochs of training has a greater potential of achieving a lower RMSE when more epochs of training are given. This assumption is not absolutely true, but it is heuristically reasonable (Jang 1996).

Using the *adaptive noise cancelling* technique, the system output serves as the error signal for the adaptive process. The system tries to reach the output trying to minimize the error. In this proposed adaptive method the input selection is done taking the channel that owns the greatest RMSE in order to choose the most uncorrelated

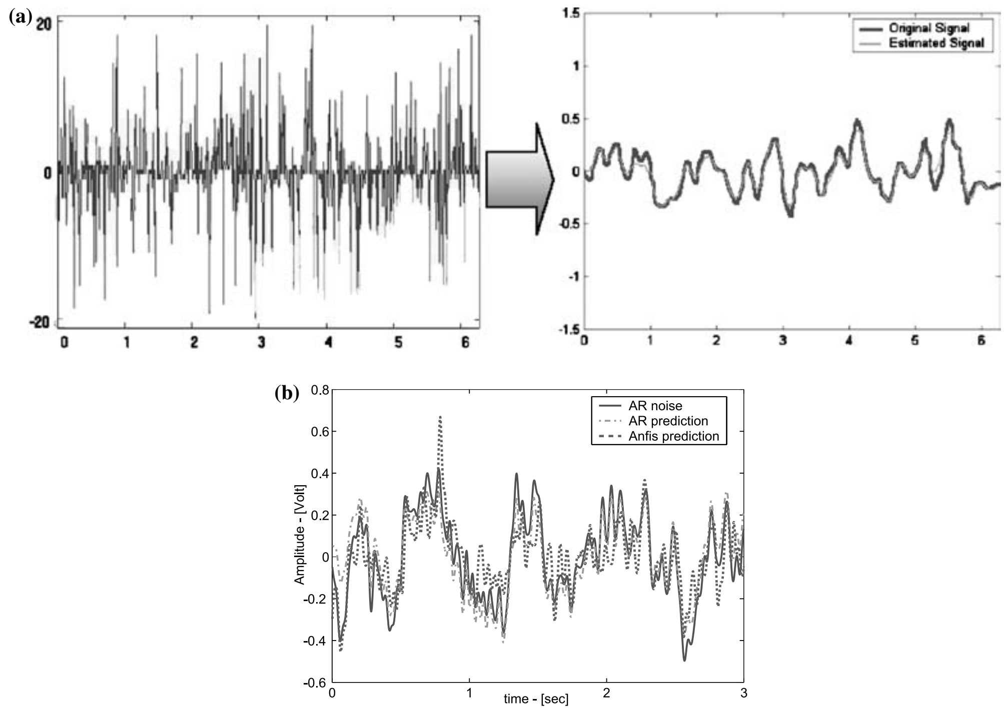

Fig. 3a, b. Simulations of the estimation capabilities of *ANFIS*. **a** *ANFIS* as noise canceller: a nonlinear corrupting function $g(n_1, n_2) = 4n_1^2 n_2^2(\sin(n_1 + n_2) + n_2)$, where n_1, n_2 are two Gaussian white noises, is added to an EEG sweep that lasts 6.25 s – $\mathrm{EEG} + g(n_1, n_2)$ *primary input* – (*left*). *ANFIS* is fed with n_1, n_2 and $\mathrm{EEG} + g(n_1, n_2)$ as inputs and trained for ten epochs over these very same inputs. The estimated noise is then subtracted from the *primary input* (*light line*). **b** *ANFIS* estimation of an AR filtered noise ("faked" EEG) compared to the estimation of an AR filter of the same order of the filter that generated the noise. *ANFIS* was used as a typical filter with the same inner membership function (mf) construction as in **b**

channel as the *primary input*. In this way we obtain the maximum possible information on the background EEG noise from the corresponding *reference* inputs. By contrast, by choosing the smallest RMSE we would choose the *primary input* with the smallest prediction error, which is the closest replica of one of the *reference* inputs because it is the signal immediately explained by a linear combination of all or some of the other sensors. In such a case, the chosen channel would be the most correlated channel of all.

In order to apply this *input selection* procedure, we alternatively take one of the four channels as the *primary input* and present it together with the other channels as *reference* input set to *ANFIS*. This way we obtain four different models, each with its particular set of inputs. We have chosen to train the *ANFIS* models for two epochs (i.e. applying twice the LS method and once the gradient descent method) before choosing the model with the best performance (i.e. different estimation errors are obtained). We accordingly select the system model that with an appropriate combination of inputs has the greatest RMSE.

2.5 Noise cancellation procedure

The adaptive neuro-fuzzy inference system (*ANFIS*) structure is trained on three input sources, which form the *reference* input set; the output of the network is compared with and adapted to the *primary input* chosen in the preceding input selection phase. Two membership functions (mfs) are associated to each of the three input nodes. The inputs correspond to four sweeps of 625 samples (250 Hz sample rate, corresponding to a sample every 4 ms).

In this case of adaptive cancelling using *ANFIS*, there is no need to improve the generalization capabilities as in typical approaches based on neural networks. The training is performed uniquely to estimate the burring noise over *one* of the sensors, only for the very specific trial over which the training is done. Therefore, we choose to train the *ANFIS* structure for 1000 epochs of trainings before obtaining the resulting fuzzy inference system with the modified (adjusted) parameters (i.e. premise parameters – the mf parameters, the consequent parameters – the linear polynomial parameters and the fuzzy-inference-system (FIS) rules). This way the FIS structure output over-fits the noise residual over the *primary input*. The over-fitting is crucial in this case of adaptive noise estimation whenever very low-amplitude signals are occluded by noise at approximately -20 dB SNRs. The estimated noise that corrupts the MRP sweep can now be subtracted from the *primary input*.

3 Simulations

To demonstrate and validate the efficiency of this method, three different simulations were performed. The first shows the ability of the algorithm to track nonlinear signals. The second one is a comparison with the well-known auto-regressive (AR) linear filter. The third one demonstrates the capabilities of *ANFIS* to reject *reference* inputs not affecting the *primary input*. All the data are shown after having applied a low-pass digital filter in the band {0, 12 Hz} (the filter used is a zero-phase FIR filter of order 30 with cut-off frequency of 12.5 Hz) since the interesting EEG signals are in this frequency range.

First simulation: Two *reference* inputs n_1, n_2 [Gaussian white noises GWN(0,1)] are generated. An EEG signal previously corrupted by a nonlinear noise $g(n_1, n_2) =$

$4n_1^2n_2^2(\sin(n_1+n_2)+4n_2)$, is the *primary input* (EEG + $g(n_1,n_2)$). $g(\bullet)$ is the nonlinear function we intend to estimate. The SNR was set to -30 dB. The left side of Fig. 3a shows the signal corrupted by the noise process; on the right the estimated signal is compared to the original signal already after ten training epochs of *ANFIS*. This simulation was performed to emphasize the capabilities of the method. This kind of chosen nonlinearity is not intended to mimic any physiological characteristics but represents an extreme case of the classical tests adopted to prove the nonlinear capability of *ANFIS*

Second simulation: We compare the ability of *ANFIS* to estimate linearly filtered noise generated simulating an AR process of order nine (Cerutti et al. 1988) (widely accepted to model EEG noise). The parameters of such an AR process were estimated from a 4-s EEG signal recording (recording site Fp1, sampling rate 512 Hz in rest condition we consider an EEG signal taken from a pre-existing database of EEG recordings). A "faked" EEG signal was obtained by filtering with the obtained filter a Gaussian noise with unitary variance and zero mean. Of course, estimating again the parameters of an AR model of the same order we obtain the best possible estimation the signal can obtain, since we are inverse filtering the filtered noise with the same filter that generated it (slight discrepancies arise between the estimated filter and the original AR filter for different methods used for optimizing the AR parameters). Nevertheless, in Fig. 3b we compare the estimation that *ANFIS* obtained with respect to an AR filter of order nine. Other simulations were run: *ANFIS* performs well even if the parameter order of the filter is unknown.

Third simulation: A set of three Gaussian white noises GWN(0,1) was considered as *reference* inputs. The *primary input* was an EEG sweep not corrupted in any way by the three noises. Therefore, a null $g(\bullet)$ was implicitly assumed. The algorithm was, accordingly, able to reject the independent noises, leaving the *primary input* unaffected.

4 Results

Considering MRPs related to left hand movements: Fig. 4b shows the estimations relevant to the third channel (whenever it was chosen as *primary input*), while Fig. 4c shows the same for the fourth channel. These curves can be compared to the averages of the third and fourth channels of the whole trial set (Fig. 4a).

Figure 5a shows a set of four plots, each representing one of the four channels, again during the movement of the left index finger. The plots are organized in topological order, reflecting the location of the four channels over the scalp. Above each plot the number of the referring channel and the number of times the channel was chosen as *primary input* are indicated. Each plot shows: (1) (heavy line) the grand average computed over all the trials of the referring channel, (2) (plain line) the average of the estimated trials (i.e. each time the channel was chosen as *primary*), (3) (light dashed line) the average of the non-denoised signals over the very same trials. Figure 5b has the same layout of Fig. 5a, but it corresponds to the movement of the right index finger. In Fig. 6 the dashed lines represent the standard deviations (SDs) of the non-denoised trials, while the plain ones represent the variability of the denoised trials, both calculated over the very same trials considered in Fig. 5a for the partial averages. It can be appreciated the decreased baseline variability of the denoised trials that permits to highlight variability peaks around the event.

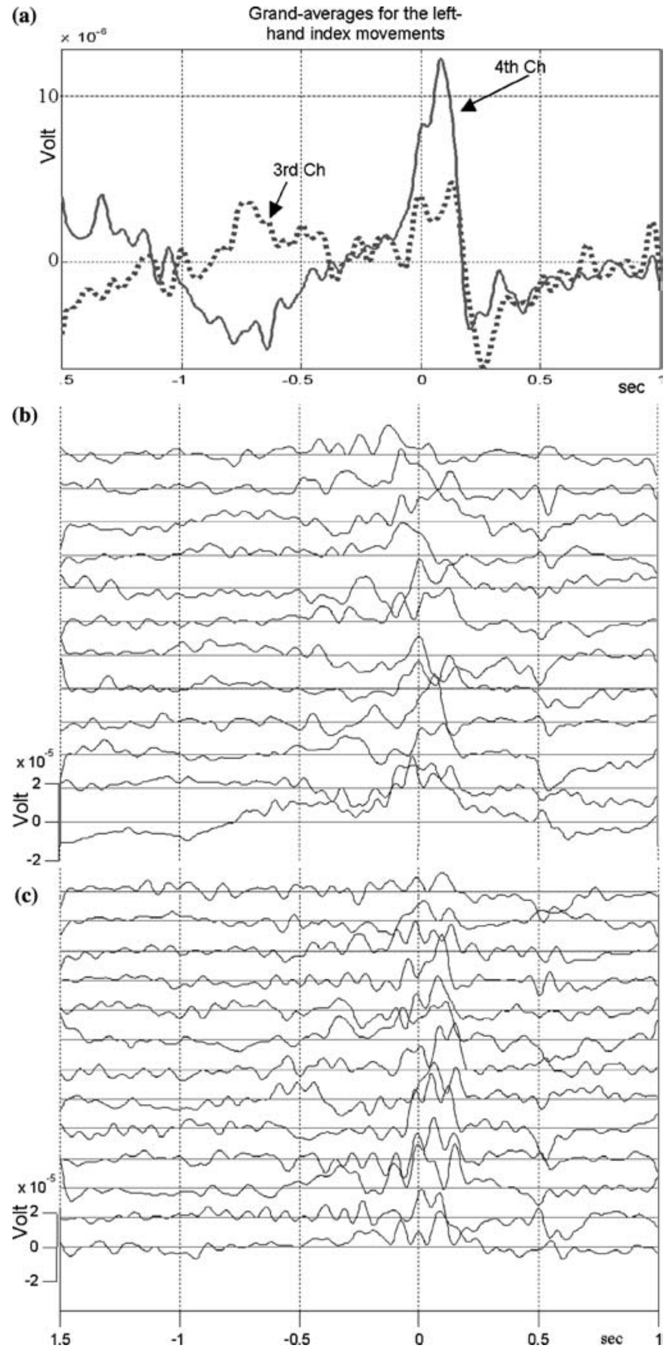

Fig. 4a–c. Left index finger movement trial set of one subject. **a** Grand averages of the third and fourth channels. **b** Single trials whenever the third channel was selected. **c** Single trials whenever the fourth channel was selected. It is interesting to note that a major phase-lock response occurs over the single-trial estimations whenever the fourth channel was selected

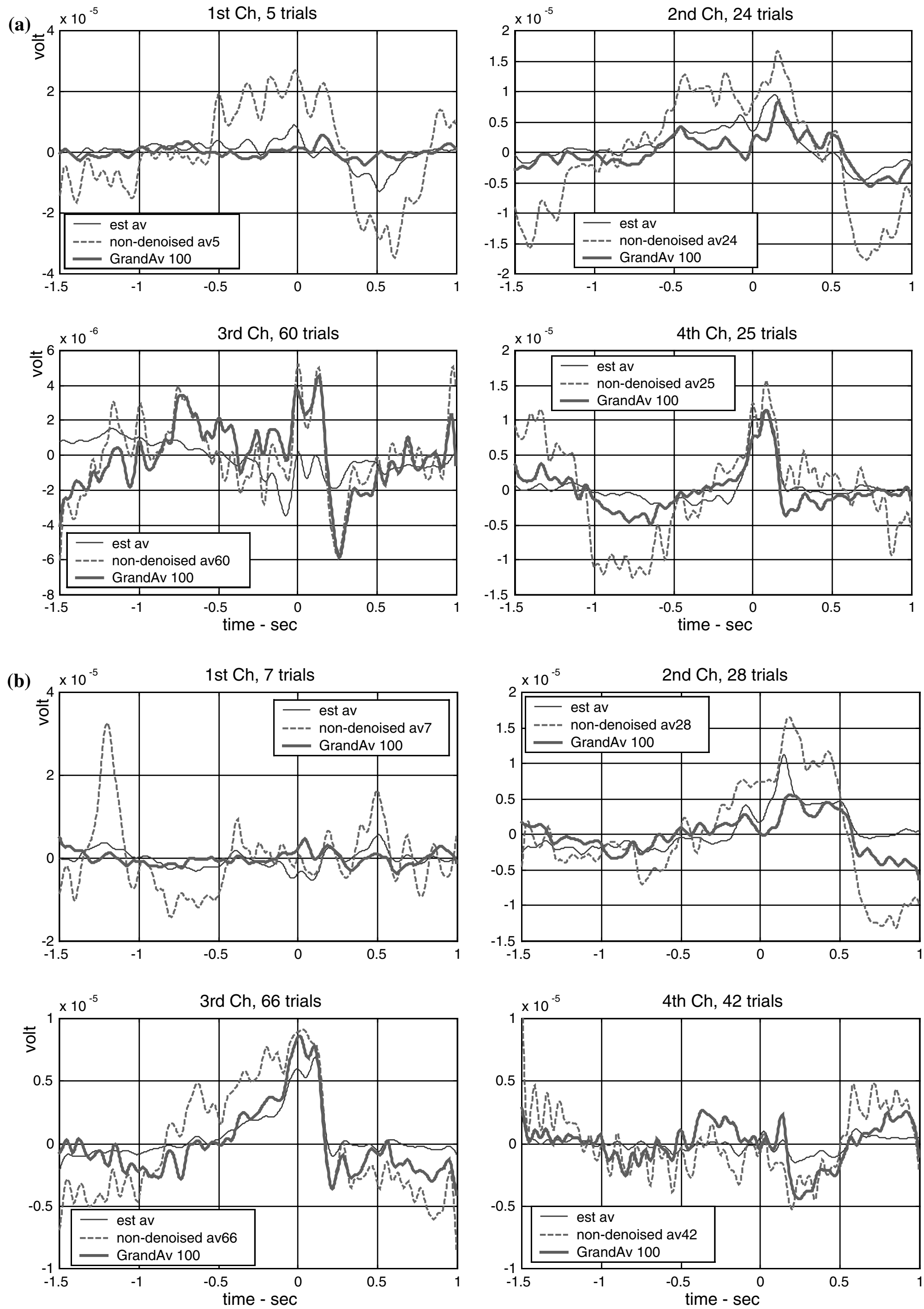

Fig. 5a, b. Averaged trends of the single-trial estimations for one subject. Each figure (reporting the *left/right* index finger movement trial set) is organized in a set of four plots. The plots are placed in topological order, reflecting the placement of the recording Laplacian filtered channels. Above each subplot are reported: the number of the referring channel and the number of times this channel was selected in its specific movement trial set. **a** *Left index finger movement trial set*: the averages of the denoised and the non-denoised single-trials over the very same trials (in which the channel was chosen for estimation) are compared to the grand averages over all the trials for each relevant channel. **b** *Right index finger movement trial set*: the same line as in **a**

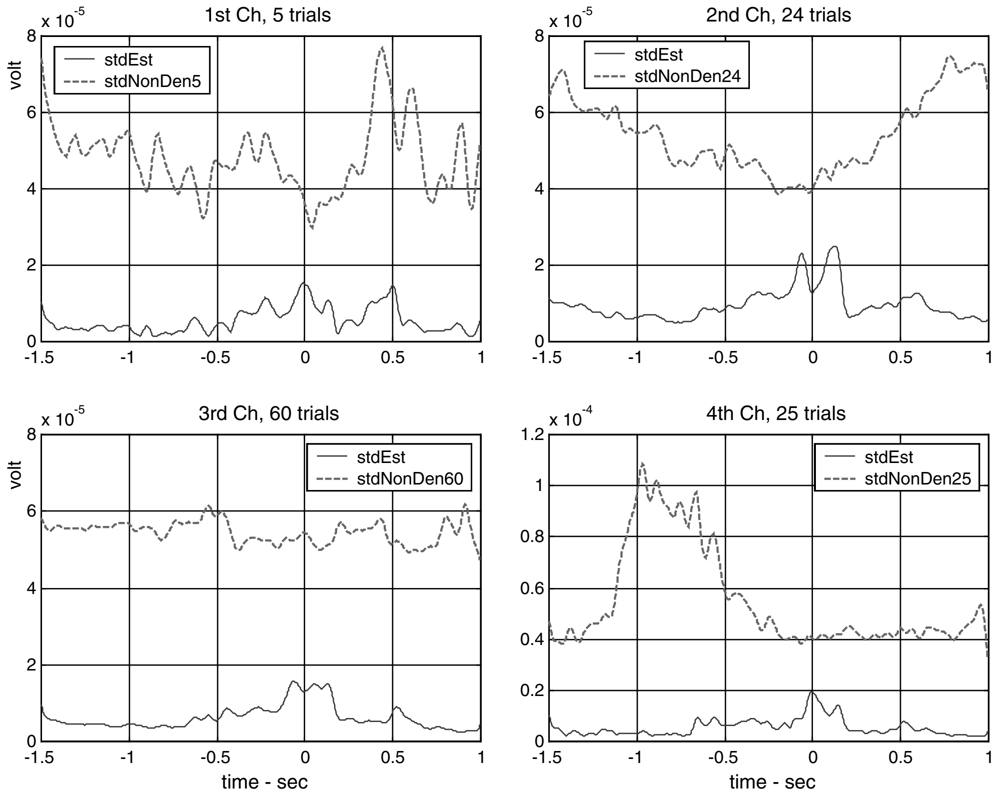

Fig. 6. Standard deviations of the denoised and the non-denoised single trials considered in Fig. 5a of the left index finger movement trial set

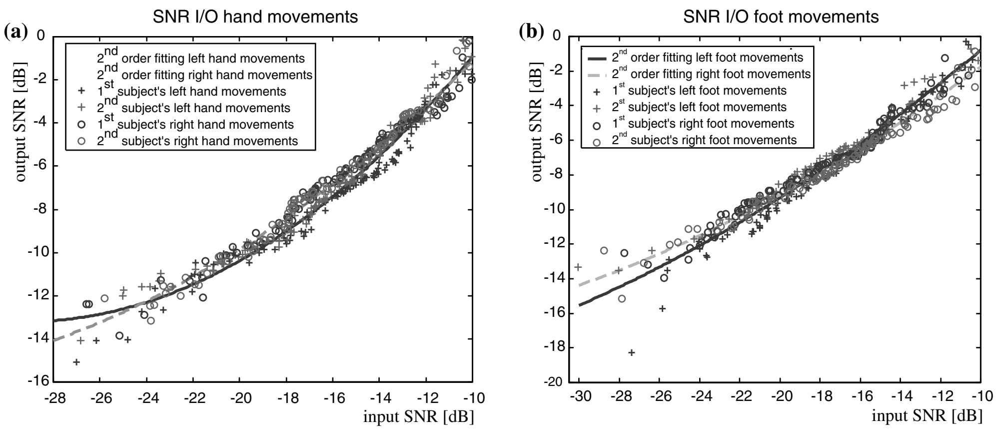

Fig. 7a, b. Method performance: input SNR vs. output (denoised) SNR (*input SNR*: ratio between the variance of the grand average and the variance of the non-denoised signal, *output SNR*: ratio between the variance of the grand average and the variance of the denoised signal). **a** Left and right index finger movement of two subjects. For each movement type a second-order polynomial fitting was plotted below the data. **b** Left and right big toe movement of two subjects

The estimation capabilities of this method are shown in Fig. 7a, where the trials relative to the movements of the right and left hands for both subjects are reported, plotting the input SNR vs. the output SNR. These two measures were computed taking for the input SNR the ratio between the variance of the grand average response and the variance of each non-denoised signal and for the output SNR the ratio between the variance of the grand average response and the variance of the denoised signal. For each movement type (left and right movements), a second-order polynomial fitting was plotted below the reported data. The data shown are in reference to all the MRP estimations in the relevant movement set independently of the chosen primary input in a specific single trial. The same considerations are valid for Fig. 7b, where the data relevant to the movement of the right and left foot are reported for both subjects.

In Fig. 8a,b the occurrences (normalized) in which each channel was chosen as *primary input* in each trial set (left and right index finger movements, left and right toe movements) are shown for both subjects.

The results of this method have been compared with other multivariate methods. Since this method does not take into account signal templates and performs the signal recovery over multi-channel data, a particularly suitable method for comparison could be independent component analysis (ICA) (Bell and Sejnowski 1995) with the natural gradient feature proposed by Amari et al. (1996). This last method is an on-line learning algorithm, which minimizes a statistical dependency among outputs and serves

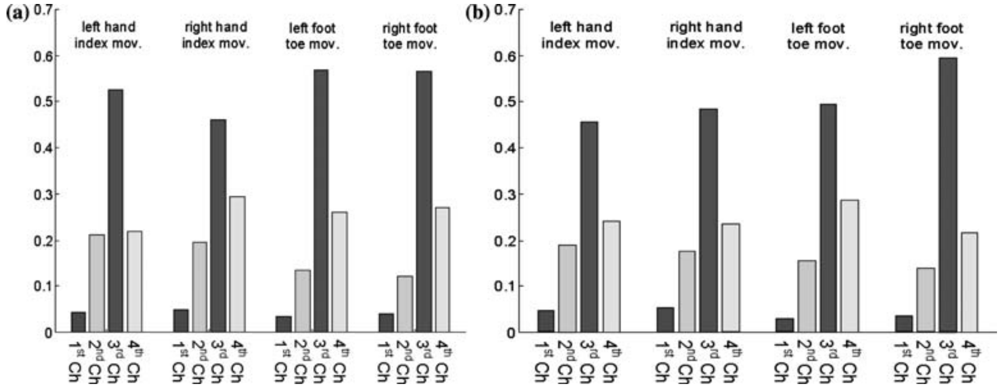

Fig. 8a, b. Percentage of occurrences in which each channel was chosen for estimation in each movement type. **a** First subject. **b** Second subject. Note the selections prefer mostly the third channel for all the movement types

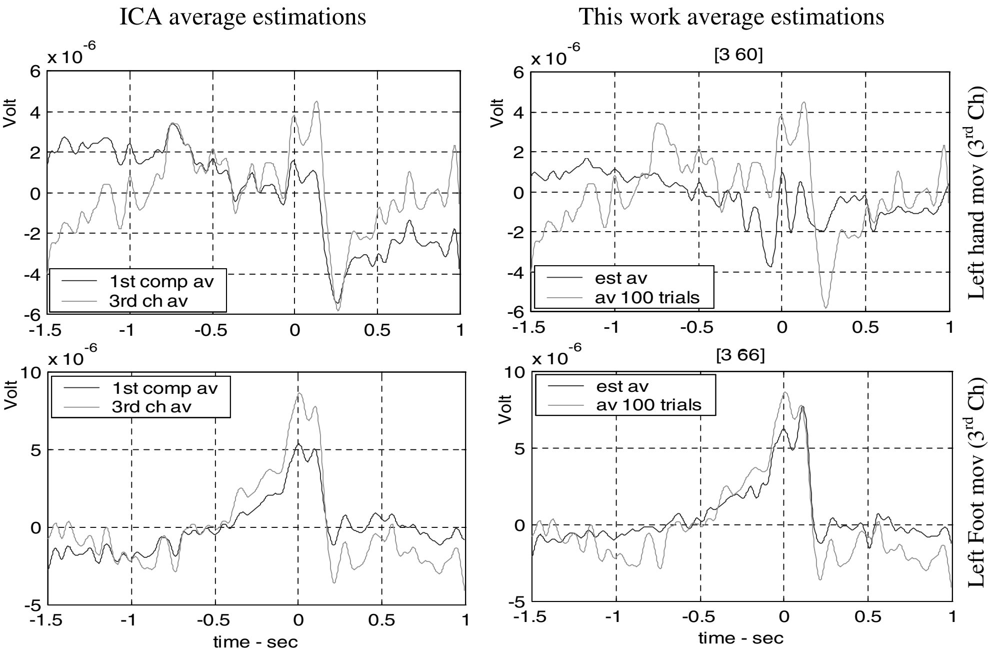

Fig. 9. Comparison between the ICA decomposition method (*left*) and the present study (*right*). The *two plots above* are relative to the movement of the left hand and the *two plots below* are relative to the movement of the right hand for one of the subjects. For both methods the grand average is plotted to permit an easier qualitative comparison between the methods

to achieve blind separation of mixed signals. The dependency is measured by the average mutual information (MI) of the outputs. The source signals and the mixing matrix are unknown except for the number of sources. The natural gradient approach is used to minimize the MI. ICA outputs a set of linearly independent signals, given a set of the original multi-channel input signals. The set of spatially Laplacian filtered signals (i.e. the same input of the present method) was served as input to ICA. Three of the four components of the ICA output were not found to be physiologically meaningful in comparison with any of the channels (correlation coefficient < 0.2). Only the first component was found, by means of averaging, to be suitable to describe the underlying MRP over the third channel (Fig. 9). The averages of the signals estimated by the two methods are plotted in Fig. 9 (ICA on the left, present study on the right); they are compared with the grand average over the third channel of the corresponding set of movements of one subject. The average of the first ICA component is computed with the same number of signals used to compute the grand average. The averages relevant to the proposed method were computed taking signals from the subset of the whole trial set (about 50%), in which the third channel was selected. Though, the averages are very similar for both methods, ICA was not able to provide significant single-trial responses, in contrast with the higher filtering capability of the proposed method (Fig. 4b,c). This result can be appreciated by comparing the SDs of the single trials in Fig. 10 for the left and right hand movements, respectively: (1) the non-denoised signals, (2) the first ICA component estimations and (3) the estimations of the present method. The variability of ICA, spread over the considered time window, does not enable MRP detection or direct analysis. Indeed, *ANFIS* filtering displays SDs of the single trials reduced by a fraction less than 1/3, compared to a fraction of more than 2/3 of ICA (Fig. 10).

For the sake of completeness and plausibility of the results presented in this paper, another cross test was made. Besides using *ANFIS* as the adaptive function in the Widrow's scheme (see Fig. 2, considering as input noise sources the channels not selected as *primary*), we inserted an ARX multivariate filter (i.e. linear dynamic model). The ARX filter is characterized by its parameters in the recursive and exogenous parts, and the general formula is given by:

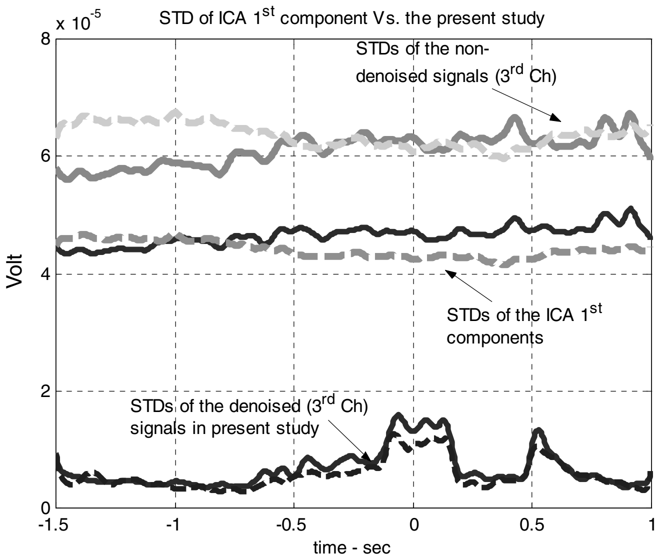

Fig. 10. Standard deviations of signals relative to the third channel of the left (*dashed lines*) and right (*thick lines*) hand movement sets of one subject. Three couples of SDs are shown: (1) the non-denoised SDs of the third channel, (2) the first ICA component SDs and (3) the SDs of the denoised signals of the present method each time they were selected. Each pair of signals is relative to (*dashed line*) left hand movements and (*thick line*) right hand movements

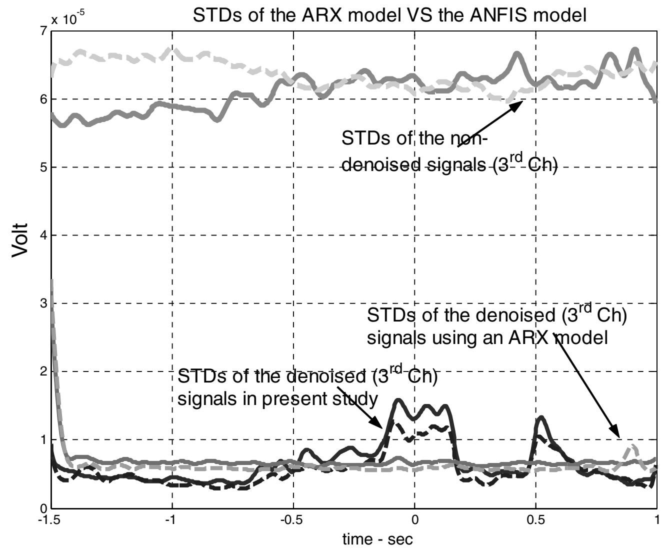

Fig. 11. Standard deviations of signals relative to the third channel of the left (*dashed lines*) and right (*thick lines*) hand movement sets of one subject. Three pairs of SDs are shown: (1) the non-denoised SDs of the third channel, (2) ARX estimation SDs and (3) the SDs of the denoised signals of the present method each time they were selected. Each pair of signals is relative to (*dashed line*) left hand movements and (*thick line*) right hand movements

$$A(q)y(n) = \mathbf{B}(q)\mathbf{u}(n) + e(n)\,,$$

where $A(q)$ is the vector of parameters of the recursive part of the filter while q is the order. **B** is the Matrix $q \times m$ of the parameters where q is the order and m is the number of exogenous inputs collected in the $\mathbf{u}(n)$ matrix. n is the length of the time series, and $e(n)$ is the white noise input of the model. The order was chosen according to the optimal Akaike order, which is equal to nine for both the regressive and the exogenous parts, and clearly this order is relative to the considered data. The test was performed to show significant differences between the two adaptive blocks (i.e. *ANFIS* and ARX); hence ARX was trained over the same training epochs used for *ANFIS* (i.e. 1000), while the parameters were adapted by means of the recursive-least-mean-squares rule. In Fig. 11 we show the results achieved by the two methods, for one subject using the same architecture scheme (Fig. 2). We have plotted, in the same way as in Fig. 10, (1) the SD of the non-denoised third and fourth channels when they were chosen as primary by the selecting procedure (see paragraph 2.5), (2) the denoised signals using *ANFIS* as adaptive block and (3) the denoised signals using ARX as adaptive block. The time-averaged SDs measured using both methods give the same result, but the SD spread over time shows that the *ANFIS* block is able to evidence the variabilities that are buried in certain time ranges [i.e. readiness potential (RP), late preparation (LP), motor potential (MP), and movement assessment]. These variabilities are of considerable interest in estimating the dynamical properties of the signal. By contrast, although the ARX model performs very well, its dynamical properties mix and merge together different components risen in different times. Moreover, since *ANFIS* is designed on both linear and nonlinear spaces, it is able to isolate and detect nonlinear components within the linear ones. The comparison shown in Fig. 11 confirms that the simple model used to explain the noise sources (e.g. see Fig. 2) is appropriate for describing and estimating the noise over the selected channel. It is important, though, to consider, in the case of implementing the proposed approach with other adaptive techniques, both the linear and nonlinear dimension spaces in order to evidence subtle variabilities in the dynamics of the signal.

5 Discussion

Linear filtering and parametric modelling methods have been widely adopted and proven to be powerful tools in recent decades (Deecke et al. 1976; Bartnik et al. 1982; Boschert and Deecke 1986; Thakor 1993), while other approaches have combined linear models and nonlinear methods (Cerutti et al. 1988; Birch et al. 1993; Thakor 1993; Wolpaw and McFarland 1994; Mason and Birch 2000); nonetheless, in recent years several studies have explored the applicability of nonlinear models and methods in exploring the information content of neurophysiological data, with a particular interest in movement-related responses, in which rapidly adapting mechanisms are elicited (Lopes da Silva et al. 1997; Dushanova and Popivanov 1996; Blanco et al. 1995; Stam et al. 1999; Sulimov 1998; Popivanov and Mineva 1999; Meyer-Lindenberg et al. 1998). Also, approaches based on principal components have been investigated (Mineva and Popivanov 1996), but their performances in separating signal features from overlapping sources were not satisfactory. It has been suggested that ICA might be more appropriate (Makeig et al. 2000). In this evolving scenario of theories and methods in the neural sciences, *ANFIS* can provide a flexible tool which shares the features of both linear filters (in its forward parameter estimate) and those of a fuzzy estimate of nonlinear characteristics (in its backward iteration stage). Another qualifying characteristic of *ANFIS* is the achievement of better results and the use of less adjustable parameters compared to other algorithms based on neural networks or on adaptive AR prediction (Jang 1993).

Generally the components of the MRP are related to the stage of the execution of the movement: early preparation [Bereitschaftspotential (BP) or readiness potential (RP), late preparation (LP), initiation (motor potential, MP), and execution of the movement or movement related response (MRR)] (Tarkka and Hallett 1991; Hallett 1994). Single trials contaminated by components of the MRPs ranged from −1,500 to −500 ms (BP), from −500 ms to zero time (LP), from zero time to +60 ms (MP), and from +60 to +120 ms (MRR) (Babiloni et al. 1999). In this study, the single-trial estimations were compared to the grand average, resulting in a very low variability trend over RP, the first part of LP and after the movement execution, while we observed a high variability surrounding movement onset (MP and execution) (Fig. 4b,c). This variability was confirmed also calculating the variance of the estimations for each set of trials (Fig. 6). We have also observed high variability peaks occurring at +500 ms, which correspond to the final subject assessment of the task (Cerutti et al. 1988). As expected, the intrinsic variability of MRP is evident in those components that are eligible to have the maximal variability, i.e. the MP and the execution of the movement itself that are typically non-phase-locked components. These components reveal the adaptation of the movement execution to the surrounding environment. The variability is observed mainly around zero time ($\sim \pm 200$ ms) and 500 ms ($\sim \pm 100$ ms) and not elsewhere, while high noise cancelling is reached even for very low SNRs. However, the model beyond this study is conceived taking information from the neighbouring channels that are supposed to carry only noise. The movement of a limb is reflected by the appearance of an MRP in all the electrodes over the motor cortex and over the prefrontal cortex. Therefore, generally (as with a more realistic approach) also the *reference* channels carry some information regarding the MRP. Cancellation of components of the estimated signal together with the cancellation of the noise is possible, especially when the movement typically activates both contra- and ipsilateral cortical hemispheres. This happens whenever the movement is relevant to the non-dominant side of the body. In Fig. 5a it is possible to notice over the plot of the third channel that the estimated average is lower than the expected one (grand average).

It remains clear that the advantages of the proposed method are that it is able to discriminate the most informative channel in each single-trial movement type and to search for nonlinear components which are not explained by the ICA method nor by the ARX filter; in addition, the method is able to minimize the variability of the signals where the MRP is actually absent (Figs. 6, 10, and 11), thus enabling detection and analysis.

Cortical excitation does not show strictly unilateral activation for all its components. For example BP preceding finger movements have been reported to have significant ipsilateral generators (Bötzel et al. 1993). In designing an automatic selection procedure of one channel among the others, we followed the evidence that MRP components are variably distributed in time and space from trial to trial. We search for the channel that is explained (in the linear/nonlinear sense) by the other channels in the worst way, assuming that it may best describe an MRP independent of the background noise. Therefore, the channel with the highest SNR (i.e. MRP/background activity) is not necessarily chosen. Interestingly, selection results relevant to left and right limb movements were not symmetric and the third (left posterior) channel was most often chosen in both cases. Thus, we shall look for a possible description of the underlying phenomenon. We should probably consider how the paradigm was administered during the trials. Subjects were told to press the bar alternating the movement of their four limbs, self-pacing and with an interval of approximately 3 s between each press. Apparently, the repetitive simple movements were accompanied by a cognitive process as the estimation of time, as in (Pelvermuller et al. 1995), and eventually the random movements of the four limbs. This cognitive process related by movements recalls the experience of Kupferman (1991) who ascertained that cognitive processes related by movements are prominent in the left hemisphere (96% in right-handed people and 70% in left-handed people). These findings may bring us to the conclusion that repertoire traces of movements are present in the left hemisphere region (contralateral to the right side body movements), but the system may or may not rely on that repertoire whenever approaching a movement task with a paradigm like the one used in this study. The left hemisphere might become highly specialized and highly precise with experience and becomes a valid and faithful repertoire to be used in determining the output of the movement system. It may be argued that this type of motor information processing is performed in the cerebellum. But as found in (Siedler et al. 2002), the motor skill itself is not learned in the cerebellum but elsewhere (rather the cerebellum is engaged primarily in the modification of performance).

6 Conclusions

The strength of the noise cancelling using *ANFIS* is the ability to track both the nonlinear and the linear relations among signals. Moreover, without any prior knowledge of the waveform, the method presented here is capable of recovering the EPs from the ongoing background cerebral activity that corrupts them with very low levels of SNR. The core of the method is based on taking the sources of the noises and of the signal directly from the system itself, avoiding use of synthetic filtered noise to estimate noises present in the system. This approach is applicable in principle to any complex noisy system of which some contemporaneous measures (of noises and signals) are available. The method was applied to recover synthetic signals previously corrupted via an unknown process by noises as well as to recover biological signals – although this represents a limited data set – achieving good results, as is illustrated in the previous sections.

This study opens a new and potentially useful window into complex event-related brain data that can complement other analysis techniques. Further research will be required to fully assess and to confirm the efficiency and limitations of the method proposed here. Other cross validations such as neurological tests might be performed. The use of electrocorticographic data in simulations for comparing the single trial MRP estimation presented in this study is a plausible best approximation of the temporal dynamics of the unknown MRP brain generators. Only such data might be the effective proof of the efficiency and reliability of this work.

Appendix

Widrow's adaptive noise cancelling

A signal is transmitted over a channel to a sensor that receives the signal plus a noise n_0; the combined signal and noise $s+n_0$ form the "*primary input*" to the noise canceller. A second sensor receives a noise n_1 which is uncorrelated with the signal but correlated in some unknown way with noise n_0. This sensor provides the "*reference* input" to the canceller. Noise n_1 is filtered to produce an output y that is a close replica of n_0. This output is subtracted from the *primary input* $s+n_0$ to produce the system output, $s+n_0-y$. Since the characteristics of the transmission paths are assumed to be unknown or known only approximately and not of a fixed nature, the use of a fixed filter is not feasible. Thus, the filter must operate under changing conditions by adjusting itself continuously to minimize the error signal. To best fit the signals, the system output is fed back to the adaptive filter, which adjusts the output through an adaptive algorithm to minimize the total system output power. In an adaptive noise-cancelling system, the system output serves as the error signal for the adaptive process. No prior knowledge on the noise n_0 or the relation between the two noises is required. The mathematical proof as a more detailed treatment for this technique can be found in (Widrow and Stearns 1985).

ANFIS

An *ANFIS* network is based on a Sugeno fuzzy model (Takagi and Sugeno 1985). This model type will be first illustrated and then placed into the framework of neural networks to enable adaptation. In the Sugeno fuzzy model, whenever an input is presented at its input node, the corresponding output is a fuzzified value, i.e. a multivalued vector. The fuzzy value is the result of the expression $x_i \in \mathbf{A}_i$, which is the grade of membership that the input x_i has within the fuzzy set $\mathbf{A}_i$. Since set $\mathbf{A}_i$ contains m mfs distributed over the dynamic range of each input x_i, the corresponding fuzzy value is an m-length vector. The combinations of each input variable membership grade with the membership grades of the other input variables generate N weights given by m^n, where n is the number of input variables. If $A_{i,j}$ is the jth mf (i.e. the mf$_{i,j}$) contained in the fuzzy set $\mathbf{A}_i$, then each weight is expressed in the following way:

$$\left(\bigcap_{h=1}^{n-i} x_h \in A_{h,i}\right) \cap \left(\bigcap_{k=1}^{i} x_{n-k+1} \in A_{n-k+1,j}\right) = w_{i,j}\ ,$$

by varying i, j independently: $i = \{1, \ldots, n\}$ and $j = \{1, \ldots, m\}$. Let $w_{i,j} = w_p$, where $p = \{1, \ldots, N\}$; the weights w_p are normalized obtaining:

$$\bar{w}_p = \frac{w_p}{\sum_{k=1}^{N} w_k}\ .$$

These N normalized weights are multiplied by N corresponding first-order polynomial functions $f_p(\mathbf{x})$, where $\mathbf{x}$ is the input vector of n elements (x_n inputs). These N operations correspond to the typical Sugeno fuzzy rule "if $\mathbf{x} \in \mathbf{A}$ then $f(\mathbf{x})$", where $\mathbf{x} \in \mathbf{A}$ contains all the N possible combinations of inputs within their corresponding fuzzy sets ($A_{i,j} \in \mathbf{A}_i \subset \mathbf{A}$). Adding the results of the N multiplications we obtain the output of the Sugeno model $g(\mathbf{x})$:

$$g(\mathbf{x}) = \sum_{p=1}^{N} \bar{w}_p f_p(\mathbf{x})\ ,$$

$$f_p(\mathbf{x}) = a_0 + \sum_{i=1}^{n} a_i \cdot x_i\ ,$$

where a_i are the linear parameters of the polynomial $f_p(\mathbf{x})$ functions. The elements of the fuzzy sets $\mathbf{A}_x$ and $\mathbf{A}_y$ are mfs that can be described by any possible 2D function. The Sugeno fuzzy model can easily adapt or learn if it is placed into a framework of adaptive neural networks that can compute gradient vectors systematically. The resultant network architecture, called *ANFIS*, is functionally equivalent to a fuzzy inference system. *ANFIS* combines two learning rules, the back-propagation (gradient descent method) and the linear LS method, obtaining a *hybrid learning* algorithm for an effective search for optimal parameters. The two learning rules are applied to the two different parts of the model. Specifically, the back-propagation adapts (recursively from the output layer backward to the input nodes) the nonlinear $w_{i,j}$ weights obtained from each rule and hence from the parameters of the intervening mfs in each fuzzy set; the LS adjust the linear a_i parameters of the polynomial functions $f_p(\mathbf{x})$ in each forward step.

References

Amari S, Cichocki A, Yang HH (1996) A new learning algorithm for blind signal separation. In: Advances in neural information processing systems, 8. MIT Press, Cambridge, MA

Babiloni C, Carducci F, Cincotti F, Rossigni PM, Neuper C, Pfurtscheller G, Babiloni F (1999) Human movement-related potentials vs. desynchronization of eeg alpha rhythm: a high-resolution EEG study. NeuroImage 10:658–665

Babiloni F, Cincotti F, Lazzaroni L, Millàn J, Mouriño J, Varsta M, Heikkonen J, Bianchi B, Marciani MG (2000) Linear classification of low-resolution EEG patterns produced by imagined hand movements. IEEE Trans Rehabil Eng 8:186–188

Bartnik EA, Blinowska KJ, Durka PJ (1982) Single evoked potential reconstruction by means of wavelet transform. Biol Cybern 67:175–181

Bell AJ, Sejnowski TJ (1995) An information-maximization approach to blind separation and blind deconvolution. Neural Comput 7:1129–1159

Birbaumer N, Ghanayim N, Hinterberger T, Iversen I, Kotchoubey B, Kübler A, Perelmouter J, Taub E, Flor H (1999) A spelling device for the paralysed. Nature 398:297–298

Birch GE, Lawrence PD, Hare RD (1993) Single-trial processing of event-related potentials using outlier information. IEEE Trans Biomed Eng 40:59–73

Blanco S, Garcia H, Quiroga RQ, Romanelli L, Rosso OA (1995) Stationarity of the EEG series. IEEE Eng Med Biol 0739/5175/95:395–399

Boschert J, Deecke L (1986) Handedness: footedness and finger and toe movement-related cerebral potentials. Hum Neurobiol 5:235–243

Bötzel K, Plendl W, Paulus W, Scherg M (1993) Bereitschaftspotential: is there a contribution of the supplementary motor area? Electroencephalogr Clin Neurophysiol 89:187–196

Cerutti S, Chiarenza G, Liberati D, Mascellari P, Pavesi G (1988) A parametric method of identification of single-trial event-related potentials in the brain. IEEE Trans Biomed Eng 35:701–711

Deecke L, Grozinger B, Kornhuber H (1976) Voluntary finger movements in man: cerebral potentials and theory. Biol Cybern 23:99–119

Dushanova J, Popivanov D (1996) Nonlinear Prediction as a tool for tracking the dynamics of single-trial readiness potentials. J Neurosci Meth 70:51–63

Hallett M (1994) Movement-related cortical potentials. Electromyogr Clin Neurophysiol 34:5–13

Jang JSR (1993) ANFIS: Adaptive-network-based fuzzy inference systems. IEEE Trans Sys Man Cybern 23(3): 665–685

Jang JSR (1996) Input Selection for ANFIS learning. In: Proceedings of the IEEE international conference on fuzzy systems, New Orleans

Kupferman I (1991) Localization of higher cognitive and associative functions. The association cortices. In: Kandel ER, Schwartz JH, Jessel TM (eds) Principles of neural science. Elsevier, New York, pp 823–838

Lange DH, Pratt H, Inbar GF (1997) Modeling and estimation of single evoked brain potential components. IEEE Trans Biomed Eng 44:791–799

Levine SP, Huggins JE, BeMent SL, Kushwaha RK, Schuh LA, Passaro EA, Rohde MM, Ross DA (1999) Identification of electrocorticogram patterns as a basis for a direct brain interface. J Clin Neurophysiol 16:439–447

Lopes da Silva FH, Pijn JP, Velis D, Nijssen PCG (1997) Alpha rhythms: noise, dynamics and models. Int J Psychophysiol 26:237–249

Makeig S, Enghoff S, Jung TP, Sejnowski TJ (2000) A natural basis for efficient brain-actuated control. IEEE Trans Rehabil Eng 8:208–211

Mason SG, Birch GE (2000) A brain-controlled switch for asynchonous control applications. IEEE Trans Biomed Eng 47:1297–1307

McFarland DJ, McCane LM, David SV, Wolpaw JR (1997) Spatial filter selection for EEG-based communication. Electroenceph Clin Neurophysiol 103:386–394

Meyer-Lindenberg A, Bauer U, Krieger S, Lis S, Vehmeyer K, Schuler G, Gallhofer B (1998) The topography of non-linear cortical dynamics at rest, in mental calculation and moving shape perception. Brain Topogr 10(4):291–299

Millàn J, Franzé M, Mouriño J, Cincotti F, Babiloni F (2002) Relevant EEG features for the classification of spontaneous motor-related tasks. Biol Cybern 86:89–95

Mineva A, Popivanov D (1996) Method for single-trial readiness potential identification, based on singular spectrum analysis. J Neurosci Meth 68:91–99

Müller-Gerking J, Pfurtscheller G, Flyvbjerg H (1999) Designing optimal spatial filters for single-trial EEG classification in a movement task. Clin Neurophysiol 110:787–798

Nunez PL (1981) Electric fields of the brain. Oxford University Press, New York

Nunez PL, Silberstein RB, Cadusch PJ, Wijesinghe RS, Westdorp AS, Srinivasan RA (1994) A theoretical and experimental study of high resolution EEG based on surface Laplacians and cortical imaging. Electroenceph Clin Neurophysiol 90:40–57

Pelvermuller F, Lutzenberger W, Preißl H, Birbaumer N (1995) Motor programming in both hemispheres: an EEG study of the human brain. Neurosci Lett 190:5–8

Pfurtscheller G, Neuper, Guger C, Harkam W, Ramoser H, Schlögl A, Obermaier B, Pregenzer M (2000) Current trends in Graz brain-computer interface (BCI) research. IEEE Trans Rehabil Eng. 8:216–219

Popivanov P, Krekule I (1983) Estimation of homogenity of a set of evoked potentials with respect to its dispersion. Electroencephalogr Clin Neurophysiol 55:606–608

Popivanov D, Mineva A (1999) Testing procedures for non-stationarity and non-linearity in physiological signals. Math Biosci 157(1–2):303–320

Schwent JR, Hillyard SA (1975) Evoked potential correlates of selective attention with multi-channel auditory inputs. Electroencephalogr Clin Neurophysiol 38(2):131–138

Siedler RD, Purushotham A, Kim SG, Uğurbil K, Willinghsm D, Ashe J (2002) Cerebellum activation Associated with performance change but not motor learning. Science 296:2043–2046

Stam CJ, Pijn JP, Suffczynski P, Lopes da Silva FH (1999) Dynamics of the human alpha rhythm: evidence for non-linearity? Clin Neurophysiol 110(10):1801–1813

Sulimov A (1998) Human scalp-recorded EEG may be a result of activity of weakly-coupled subsystems. Neurosci Lett 250(1):72–74

Takagi T, Sugeno M (1985) Fuzzy identification of systems and its applications to modeling and control. IEEE Trans Sys Man Cybern 15:116–132

Tarkka M, Hallett M (1991) Cortical topography of premotor and motor potentials preceding self-paced, voluntary movement of dominant and non-dominant hands. Electroenceph Clin Neurophysiol 75:36–43

Thakor NV (1993) Adaptive filtering of evoked potentials. IEEE Trans Biomed Eng 40:6–12

Widrow B, Stearns D (1985) Adaptive signal processing. Prentice-Hall, Englewood Cliffs, NJ

Wolpaw JR, McFarland DJ (1994) Multichannel EEG-based brain–computer communication. Electroenceph Clin Neurophysiol 90:444–449